Microstructures from a Mixture of ABC 3-Miktoarm Star Terpolymers and Homopolymers in Two-Dimensional Space

Dazhi Kou,[†,‡] Ying Jiang,[†,‡] and Haojun Liang*[,†,‡]

Hefei National Laboratory for Physical Sciences at Microscale and Department of Polymer Science and Engineering, University of Science and Technology of China, Hefei, Anhui, 230026, People's Republic of China

Received: June 13, 2006; In Final Form: September 17, 2006

Using a 2D real-space self-consistent field theory, we studied the microstructures of the mixture of ABC 3-miktoarm star terpolymer and linear homopolymers. First, we found that the microstructures depend on both the chain length and volume fraction of the linear homopolymer. Second, despite different linear homopolymer lengths, all the mixtures finally converge to the core/shell pattern after the sum of blocks and homopolymer comprises the majority. Third, some novel microstructures that are not found in the pure ABC 3-miktoarm star terpolymer are produced. These calculations are supposed to be helpful for the design of novel microstructures involving star terpolymers that blend with homopolymer.

1. Introduction

To fulfill the industry's requirements, scientists endeavor to find simple and efficient approaches to manufacturing novel materials. Polymeric nanomaterials, usually manufactured via self-assembly of block copolymers, are currently proven to have potential applications in the design of nanodevices, such as photonic crystal. Usually, most attempts focus on synthesizing more complex block copolymers, i.e., complex chemical structures of monomers or the architecture of a block copolymer chain. One expects that the block copolymer chains having such complicated structures could also be assembled into materials having novel microstructures. However, synthesizing those complex block copolymers will take high skill, more effort, and large funds to support. Currently, we noticed that in the late 1980s, plastic alloys, which were made by simply blending two kinds of polymers, had been widely applied to many industrial aspects because of their super properties. Inspired by this idea, the present study shall investigate the microstructures assembled via the mixture of block copolymers and homopolymers. We would like to observe whether some novel structures can be found in these mixtures. If this method proves to be promising, it should be readily accomplished industrially.

Multicomponent polymeric materials, such as diblock or triblock copolymers formed by various chemically linked homopolymer chains, are mostly thermodynamically incompatible. This property enables these soft materials to have the ability to phase separate and self-assemble into a rich variety of microstructures (typically with domain scales from 10 to 100 nm).[1] This fascinating property attracts the attention of polymer chemists and material physicists. The simplest block copolymer is a linear AB diblock copolymer: the segment−segment interaction energy (χ) and the chain-stretching-driven changes in entropy cause block copolymers to separate into well-ordered structures below an order−disorder transition determined by the product χN, where N is the degree of polymerization. There are four stable ordered structures that have been published,[2−4] namely, lamellae, gyroids, cylinders, and spheres. Recently, Tyler and Morse theoretically predicted the fifth stable structure O^{70}, which is within a narrow and very weakly segregated region and competes closely with the gyroid phase; it is not, however, observed in the experiment owing to fluctuation effects.[5] In the last few decades, a great deal of experimental and theoretical effort has been spent on the study of diblock copolymers; the phase behaviors of these simple systems are now well understood. Although diblock copolymers provide a rich phase behavior and five ordered phases, it remains desirable to search for the possibility of producing more varied phases from block copolymers. There are two ways to carry out this goal. One is to enlarge the types of monomers present in the block copolymers. The simplest approach toward this direction is to study the ABC triblock copolymer systems. Relative to their corresponding AB diblock copolymers, significant increases occur in both the complexity and variety of structures that are self-assembled from ABC triblock copolymers, i.e., upon increasing the number of distinct blocks from two to three.[6−12] These three blocks cannot only form a linear chain, but more interestingly, they can also have a starlike form by joining three block ends in one junction point. Compared to linear triblock copolymers, this junction point limitation gives another entropic effect in a star triblock copolymer. Qiu et al.[11] and Liang et al.[12] systematically investigated the morphology of an ABC star triblock copolymer, and nine microphases were found to be stable, including hexagonal lattice, core−shell hexagonal lattice, lamellae, and lamellae with beads at the interface, etc. Furthermore, as far as experiment is concerned, it is easier to blend multicomponents. In this method, different block copolymers or homopolymers are mixed to produce ordered phases.[13−24] Matsen studied diblock copolymers blending with homopolymers;[23] Shi et al.[24] studied the blending of triblock and diblock copolymers, especially the addition of homopolymers to copolymers, to form an analogy to the amphiphile−water system.[23]

There are different theoretical tools used to investigate the microphase formation of block copolymers, such as Monte Carlo simulations by Gemma et al.[25] and molecular dynamic simula-

* Address correspondence to this author. E-mail: hjliang@ustc.edu.cn.
† Hefei National Laboratory for Physical Sciences at Microscale.
‡ Department of Polymer Science and Engineering.

10.1021/jp063695k CCC: $33.50
Published on Web 10/28/2006

tions by Schultz et al.[26] In previous work, we have investigated microstructures through the assembly of ABC 3-miktoarm star terpolymers and linear homopolymers using dynamic density functional theory (DDFT).[27] However, these methods are difficult in terms of numerical computation, since only a few points in the parameter space are touched. Another powerful technique for characterizing the polymeric systems is carried out to study phases and phase transitions. This is called the self-consistent field theory (SCFT). SCFT is a mesoscopic simulation technique formulated by Edwards in the 1960s and adapted by Helfand and others, explicitly for the study of block copolymers. This technique has been extremely useful for studies of inhomogeneous polymers and complex fluid phases.[28−34] The application of such methods to dense phases, such as melts and concentrated solutions of homo, block, and graft copolymers, has been particularly fruitful for unraveling the complexities of their self-assembled structures at equilibrium. Matsen and Schick[30] have solved the SCFT equation successfully using the "spectral" approach. This method is numerically efficient and allows high-precision calculations of free energies and phase diagrams, but it has a flaw in that it requires that the relevant morphologies must be known a priori. To circumvent this problem, Drolet and Fredrickson recently suggested the implementation of SCFT for monodisperse block copolymers, where low free energy morphologies are found through relaxation from random potential fields.[32−34] A similar real-space approach has also been suggested by Bohbot-Raviv and Wang.[35] In this article, we use real-space SCFT to investigate microstructures in blending star triblock copolymers and homopolymers.

2. Theoretical Method

We consider an incompressible blend of linear homopolymers and ABC triblock copolymers in a volume V. The total degree of polymerization of the triblock is N; for the homopolymer, it is αN (thus, α is the ratio of the degree of polymerization of the homopolymer to that of the triblock). The triblock consists of an a-block, a b-block, and a c-block, having a degree of polymerization of $f_{3A}N$, $f_{3B}N$, and $f_{3C}N$, respectively. The triblock composition variables satisfy $f_{3A} + f_{3B} + f_{3C} = 1$. We scale distances by the Gaussian radius of gyration: $R_{g0} = a(N/6)^{1/2}$. The monomer statistical Kuhn length a and the bulk monomer density ρ_0 are assumed to be the same for all three chemical species. In the paragraph below, we will scale the chain length by the homopolymer degree of polymerization N.

Each star polymer is parametrized with the variable s, which increases along each arm. The core of the star corresponds to $s = 0$. Along the A arm, s increases from 0 at the core to $f_{3A}N$ at the outer end. The B and C arms are parametrized similarly. With these definitions, the polymer segment probability distribution functions $q_K(r,s)$ and $q_K^+(r,s)$ for species K satisfy the modified diffusion equations:

$$\frac{\partial q_K(r,s)}{\partial s} = \frac{a^2}{6}\nabla^2 q_K(r,s) - \omega_K(r) q_K(r,s)$$

$$\frac{\partial q_K(r,s)}{\partial s} = \frac{a^2}{6}\nabla^2 q_K(r,s) - \omega_K(r) q_K(r,s) \qquad (1)$$

where a is the Kuhn length of the polymer segment, $\omega_K(r)$ is the self-consistent field for species K, and $0 < s < f_K$. The initial conditions are $q_K(r,0) = q_L^+(r,0)q_M^+(r,0)$ and $q_K^+(r,f_K) = 1$, where $(KLM) \in \{(ABC),(BCA),(CAB)\}$. Note that one must solve for $q_K^+(r,s)$ prior to solving for $q_K(r,s)$. Accordingly, the partition function of a single triblock copolymer chain interacting with the mean field $\omega_K(r)$ can be written as $Q_3 = \int dr q_K(r,s)\, q_K^+(r,s)$ in terms of $q_K(r,s)$ and $q_K^+(r,s)$. We note that Q_3 is independent of the contour length parameter of a chain, s. For the homopolymer, its single chain partition function is $Q_1 = \int dr q_1(r,\alpha)$, where $q_1(r,0) = 1$ and

$$\frac{\partial q_1}{\partial s} = \frac{1}{6}Nb^2\nabla^2 q_1 - \omega_I(r) q_1$$

where the blends consist of n_c ABC triblock copolymers of polymerization index N and n_1 I homopolymers (I = A, B, C) of index αN.

Beginning with the many-chain Edwards Hamiltonian, we can derive the free energy F of the blend in the mean-field approximation. The suitably scaled free energy density f at temperature T is given by eq 2 as follows:

$$f \equiv \frac{NF}{\rho_0 V k_B T} = \frac{1}{V}\int dr\{\chi_{AB}N\phi_A(r)\phi_B(r) + \chi_{AC}N\phi_A(r)\phi_C(r) + \chi_{BC}N\phi_B(r)\phi_C(r) - \xi(1 - \phi_A - \phi_B - \phi_C) - \sum_{I=A,B,C}\omega_I(r)\phi_I(r)\} - e^{\mu_1}Q_1[\omega] - Q_3[\omega] \qquad (2)$$

We derive eq 2 using the grand canonical ensemble. Multiple phase coexistence, which we will encounter below, is most conveniently studied by using this ensemble. μ_1 is the chemical potential for the homopolymer, in units of k_BT. Since the blend is incompressible, the chemical potential for the triblocks can be set to zero without loss of generality. ϕ_A, ϕ_B, and ϕ_C are the monomer density fields normalized by the local volume fractions of A, B, and C, respectively; ω_A, ω_B, and ω_C are the conjugate fields while χ_{ij} is the Flory−Huggins interaction parameter between species i and j. $\xi(r)$ is the potential field that ensures the incompressibility of the system, which is also known as a Lagrange multiplier. Minimizing the free energy in eq 2 with respect to ϕ_A, ϕ_B, ϕ_C, ω_A, ω_B, ω_C, and ξ leads to the following self-consistent field equations that describe the equilibrium morphology:

$$\omega_A(r) = \chi_{AB}\phi_B(r) + \chi_{CA}\phi_C(r) + \xi(r) \qquad (3)$$

$$\omega_B(r) = \chi_{AB}\phi_A(r) + \chi_{BC}\phi_C(r) + \xi(r) \qquad (4)$$

$$\omega_C(r) = \chi_{CA}\phi_A(r) + \chi_{BC}\phi_B(r) + \xi(r) \qquad (5)$$

$$\phi_A(r) + \phi_B(r) + \phi_C(r) = 1 \qquad (6)$$

$$\phi_A(r) = \int_0^{f_A} ds q_A(r,s) q_A^+(r,s) + e^{\mu_2}\int_0^{\alpha} ds q_1(r,s) q_1(r,\alpha - s) \qquad (7)$$

$$\phi_B(r) = \int_0^{f_B} ds q_B(r,s) q_B^+(r,s) \qquad (8)$$

$$\phi_C(r) = \int_0^{f_C} ds q_C(r,s) q_C^+(r,s) \qquad (9)$$

In eqs 7−9, we take the case of the blended homopolymer as A. We solved eqs 3−9 directly in real space by using the combinatorial screening algorithm proposed by Drolet and Fredrickson.[32,33] This method involves a search for low free energy solutions of the equations within a planar square or box having a periodic boundary condition. The relaxation scheme for calculating the saddle-point values for the fields is implemented through the following steps:

(1) Define a uniform grid within the calculation cell. Set the initial values of ω_A, ω_B, and ω_C at every point on the grid by using a random number generator.

(2) The modified diffusion equations are solved numerically by using a "pseudospectral method"[36,37] to calculate $q(r,s)$ and $q^+(r,s)$.

(3) Numerically evaluate the integrals of eqs 7−9 for ϕ_A, ϕ_B, and ϕ_C.

(4) The chemical potential field ω_I can be updated by using the equation $\omega_I^{new} = \omega_I^{old} + \Delta t(\delta F/\delta\phi_I)^*$, where $(\delta F/\delta\phi_1)^* = \sum_{M\neq 1}\chi_{IM}(\phi_M(r) - f_M) + P(r) - \omega_I^{old}$ as the chemical potential force.

(5) The effective pressure field, $\xi = C_2C_3(\omega_A + \omega_B) + C_1C_3(\omega_B + \omega_C) + C_1C_2(\omega_A + \omega_C)/2(C_1C_2 + C_2C_3 + C_1C_3)$, on each grid is obtained through solving eqs 3−6, where $C_1 = \chi_{CA} + \chi_{BC} - \chi_{AB}$, $C_2 = \chi_{CA} + \chi_{AB} - \chi_{BC}$, and $C_3 = \chi_{AB} + \chi_{BC} - \chi_{CA}$.

The numerical calculation is performed in the two-dimensional (2D) cell having periodic boundary conditions. Because the final morphologies can be influenced by the calculation box size,[35] two types of methods are commonly used to change the box size to minimize the free energy: (I) the cubic calculation cell shape is fixed and the cell size is adjusted[37] or (II) the cell size and shape are both adjusted.[10,38] In our calculation, we use the former method, i.e., $L_x = L_y$ is fixed and the size of the lattice spacing dx (and dy) is adjusted, so that $\partial F(\delta x_{min})/\partial(\mathrm{d}x) = 0$. The average chain length of the polymers is fixed at $N_n = 90$. Noticeably, for the modified diffusion eq 1, the pseudospectral method provides a higher accuracy $(\Delta s)^3$ than the Crank-Nicholson method[10] $(\Delta s)^2$, and Δs is 0.01 in the present system. Next, we perform the simulation for each sample until the phase pattern is stably invariable with time and $\Delta F < 10^{-6}$. Obviously, the results presented in this paper are subject to the 2D model, and, hence, may not necessarily be applied to the solution of those intrinsic 3D structures. The results obtained from the 2D model, however, have a large range of potential applications, including use on nanolithographic templates and membranes, and as precursors for quantum electronic arrays. Moreover, even in a 3D system, the microphases having translational invariance along certain directions, such as lamellar and cylindrical phases, can also be investigated by using a 2D model.

3. Results and Discussion

Our focus is the phase behaviors of an ABC 3-miktoarm star terpolymer blended with homopolymers. The chain length of terpolymers is fixed at 90 and the three arms (A, B, and C) of terpolymers have equal chain length, i.e., 30 beads for each arm. Linear homopolymers with molecular length 10, 30, 60, 90, and 120, respectively, are blended with terpolymers. The calculation was carried out via increase of homopolymer's volume fraction by 1% each time. The interaction parameters are set to be $\chi_{AB}N = \chi_{BC}N = 2\chi_{AC}N = 36$.

To understand the change of the phase after addition of homopolymers, we first depict the phase diagram of pure ABC 3-miktoarm star terpolymers. Its difference from a diblock copolymer is that for a three-component system, it is difficult to depict all of the possible microstructures in a single phase diagram because the microstructures are determined by a total of five independent variables. But we can draw a three-component triangle phase diagram (Figure 1) by observing the dependence of the microstructures on the components of the three blocks having invariant interaction energies between distinct blocks, as Qiu et al.[10] and Jiang et al.[12] previously depicted the phase diagrams in this manner. As displayed in

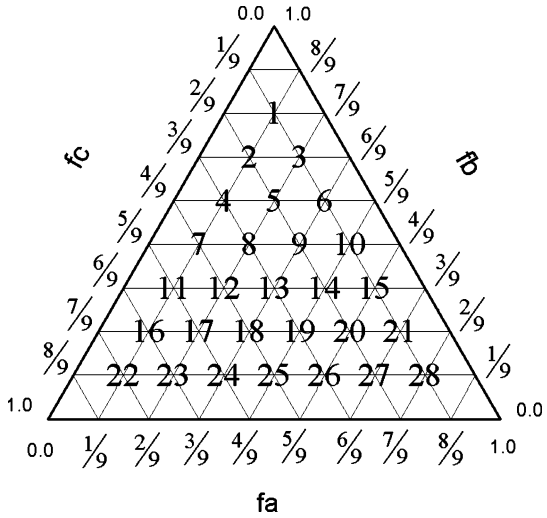

Figure 1. The locations within the phase diagram: numbers 1−28 correspond to the morphologies of the phases in Figure 2. The coordinates f_a, f_b, and f_c represent the volume fractions of the A, B, and C blocks, respectively.

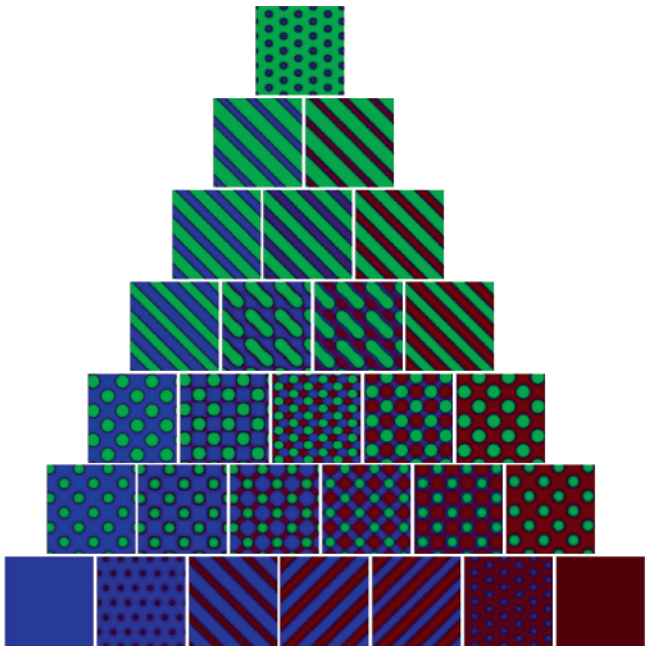

Figure 2. Phase diagram of ABC 3-miktoarm star terpolymers having binary interaction parameters $\chi_{AB}N = \chi_{BC}N = 2\chi_{AC}N = 36$. The red, green, and blue regions represent the density distributions of the monomers belonging to the A, B, and C blocks, respectively.

Figure 2, the phase diagram corresponds to the interaction parameters $\chi_{AB}N = \chi_{BC}N = 2\chi_{AC}N = 36$. The red, green, and blue regions represent the density distributions of the monomers belonging to A, B, and C blocks, respectively. According to the interaction parameters, A and C components should be symmetrical in this diagram to the line along which the B monomers have an equal volume fraction. For example, the patterns in numbers 12 and 14 in Figure 2 are identical if we exchange the red (A component) and the blue (C component) colors. The aim of the choice of these interaction parameters, i.e., $\chi_{AB}N = \chi_{BC}N = 2\chi_{AC}N = 36$, is to allow components A and C to be relatively compatible among the three incompatible components. Nevertheless, it is hoped that some distinct microstructures after blending pure A (or C) with B homopolymers can be observed.

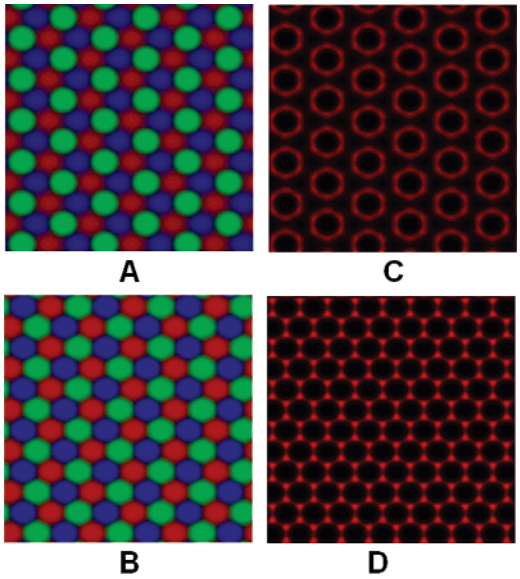

Figure 3. Microstructures of ABC 3-miktoarm star terpolymers with binary interaction parameters: (A) $\chi_{AB}N = \chi_{BC}N = 2\chi_{AC}N = 36$; (B) $\chi_{AB}N = \chi_{BC}N = \chi_{AC}N = 36$. C and D represent the corresponding junction-point distribution for parts A and B, respectively.

The diagram shown in Figure 2 can be clustered into seven typical microstructures: I, hexagonal lattice (corresponding to the position at number 1 in Figure 1); II, lamellar phases (numbers 2, 3, 4, 5, 6, 7, 10, 24, 25, and 26); III, hexagonal honeycomb lattice (number 13); IV, broken lamellar phases (numbers 8 and 9); V, core/shell tetragonal lattice (numbers 11, 15, 16, 21, 23 and 27); VI, interpenetrating tetragonal lattice (numbers 12, 14, 17 to 20); and VII, disorder phases (numbers 22 and 28).

The microstructures in this diagram can be understood as follows. We start from the pattern at number 13, i.e., corresponding to chains with equal length for the three blocks. As displayed in Figure 2 at number 13 and Figure 3A (Figure 3A is the enlargement of number 13 in Figure 2), these ABC 3-miktoarm star terpolymers assemble into the hexagonal honeycomb lattices. As indicated in Figure 3B, these hexagonal honeycomb lattices extremely resemble the ones assembled from the similar ABC 3-miktoarm star terpolymers but having three equal but highly incompatible components ($\chi_{AB}N = \chi_{BC}N = \chi_{AC}N = 36$). In Figure 3B, we may notice that each individual domain in the system containing highly incompatible components ($\chi_{AB}N = \chi_{BC}N = \chi_{AC}N = 36$) is hexagonal-like, the junction points are distributed inhomogeneously on the intermaterial dividing surface (IMDS) (Figure 3D), resembling our previous observation.[39] From Figure 3A, we can observe that the domains formed by A and C components [red and blue] are hexagonal-like, their interfaces are somewhat blurry because of the relatively weaker impulse between these two components. However, the domains of the B component are arranged in a circle (Figure 3A). The arrangement of the B block in such way is to lower the system energy by reducing the contact area with the other two components, i.e., sphere (circle) having the minimum surface area (length) for a constant volume (area) system. Furthermore, the most distinct feature of the system is that the junction points shown in Figure 3C are distributed homogeneously around domains of component B, and are absent

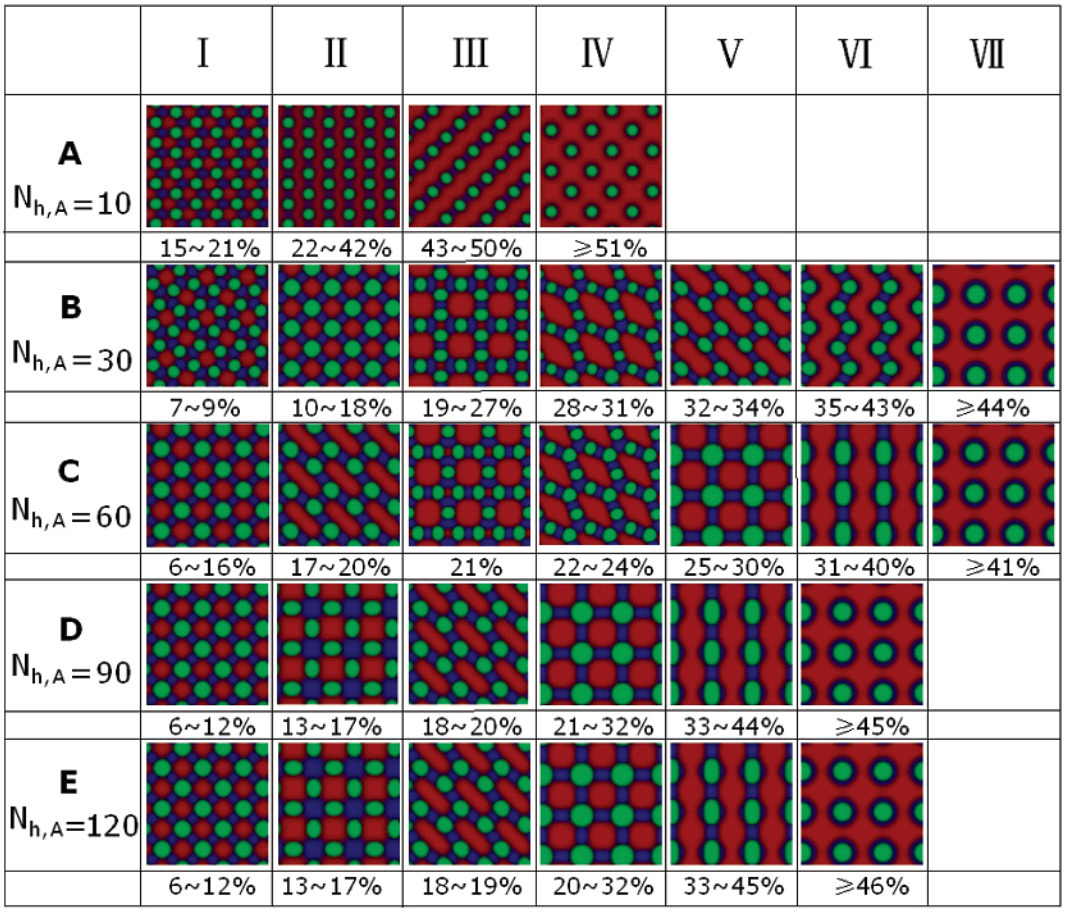

Figure 4. The microstructures assembled via the mixture of ABC 3-miktoarm star terpolymers with linear A homopolymers having varied molecular length $N_{h,A}$. The total molecular length (sum of the length of three blocks) of star terpolymer is $N = 90$, the binary interaction parameters are $\chi_{AB}N = \chi_{BC}N = 2\chi_{AC}N = 36$. The numbers at the bottom on each panel are the volume fraction of homopolymers.

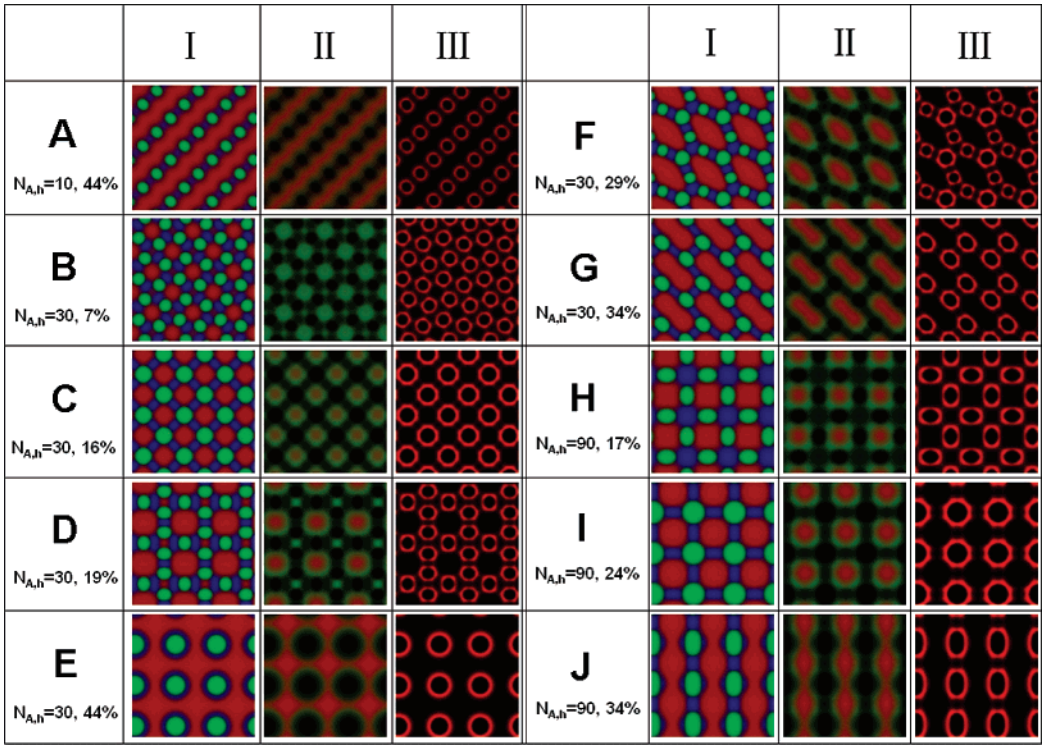

Figure 5. Density distribution of monomers belonging to the three kinds of component (I), A component (II), and junction points (III) after addition of different quantities of A homopolymers having varied molecular length ($N_{A,h}$). In column I, red, green, and blue represent A, B, and C components, respectively. In column II, red and green represent A homopolymer and A block on the ABC 3-miktoarm terpolymers, respectively.

on the interfaces between components A and C. The domains are arranged in such a manner as to avoid the direct connection between components B with two other components in order to lower the system energy.

On the basis of the above analysis, we can also understand other microstructures in this system. For instance, the hexagonal honeycomb lattices cannot be maintained after variation of the volume fraction of three components. Because of the homogeneous distribution of junction points in the interfaces around B domains, the short A blocks, which cannot be stretched too far away from the junction points, will be distributed near the interfaces, while the long C blocks can be distributed in the space somewhat far away from the interface. As a result, A core/shell patterns (see numbers 11 and 16 in Figure 2) or lamella patterns (numbers 2, 4, and 7 in Figure 2) produced by short A blocks reside homogeneously on the surfaces of the B domains. Relative to the pattern in number 11, after further increasing the A block length, some of the A blocks are used to cover the surface of B domains, and the remaining ones will be aggregated into the interpenetrating tetragonal lattice (number 12 in Figure 2). Comparing the patterns in numbers 12 and 13, we notice that the volume of the individual B domain in number 12 is twice as large as that in number 13. To explain this phenomenon, we may indicate that it will take more A blocks to totally cover the surface of domain B because of the smaller size of domain B in number 13 (in the constant volume, smaller domains will possess larger surfaces). But when the A block length corresponding to the case in number 12 is not long enough, the two B domains will aggregate into a bigger one to reduce the surface areas of the B domains.

3.1. Addition of A Homopolymers. We first add a few percentage of A homopolymer into pure ABC miktoarm block copolymers. As shown in Figure 4, the microstructures assembled via the mixture of these two types of polymers, i.e., ABC miktoarm terpolymer and A homopolymers, have the following features: (1) the microstructures depend both on addition volume fraction and homopolymer length; (2) despite different homopolymer length A, all the mixtures finally converge to a core/shell pattern after component A, the sum of block A, and homopolymer A become the majority, similar to that in number 21 in Figure 2; (3) some novel microstructures produced are not found in the pure ABC 3-miktoarm star terpolymer (comparison of Figures 2 and 4); and (4) when the length of homopolymer A is comparable to that of block A in the ABC 3-miktoarm terpolymer, such as $N_{h,A} = 30$ and 60, the system exhibits more rich patterns.

The detailed analysis in Figures 4 and 5 reveals that the B domain always displays in a circle-like or an ellipse-like structure as its component comprises only the minor part, and the junction points are always distributed homogeneously on the interface around the B domain. The system adjusts its structure in such a manner as to lower the interfacial energy via reducing the interfacial area and preventing direct contact of the B domain with the other two components.

Figure 4A reveals that as the volume fraction of addition is less than 21%, the dispersed phases formed via A blocks on the star terpolymers are mainly swollen by those homopolymers. After the volume fraction of addition exceeds 21%, the linear homopolymers, together with the A blocks on the star terpolymer, form a continuous phase, first in the lamella-like ($<$50%) then in the core/shell-like ($\geq$51) phase (Figure 4A). We notice that the B domains remain almost the same in size as they appear in number 13 of Figure 2, i.e., the size of domain B does not change with the addition of linear homopolymer.

Next, by adding linear homopolymers whose chain length is comparable to that of the corresponding block (A block on the star terpolymer), we observe from Figure 4B that the swollen dispersed phases formed via linear homopolymer A and blocks A have a strong tendency to maintain their present dispersed phasese and they do not easily aggregate into the continuing

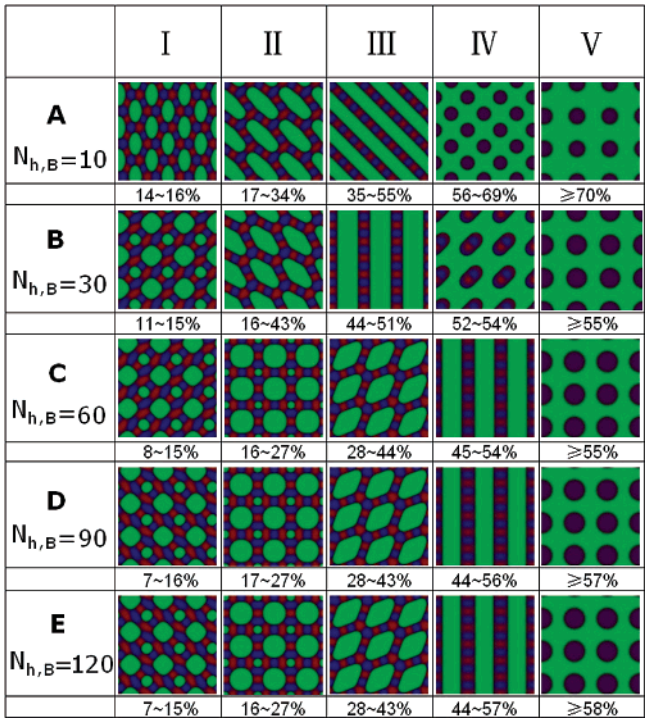

Figure 6. The microstructures assembled via the mixture of ABC 3-miktoarm star terpolymers with linear B homopolymers having varied molecular length of $N_{h,B}$. The total molecular length (sum of the length of three blocks) of star terpolymer is $N = 90$, and the binary interaction parameters are $\chi_{AB}N = \chi_{BC}N = 2\chi_{AC}N = 36$. The numbers at the bottom of each panel are the volume fraction of homopolymers.

phase as they do in the case of adding short chain (Figure 4A). The lamellar-like phase starts to form up to an additional volume fraction of up to 35%. Figure 5 shows that additional linear homopolymers prefer to reside in the central area of swollen A domains, while the A blocks on the star terpolymers stay near the interfaces around these swollen A domains, i.e., these linear homopolymer domains are covered by the shell of A blocks. Thus, the larger domain of A homopolymers needs more A blocks to totally cover, i.e., without exposing the surface of domains formed by A homopolymers. As seen in Figure 4B, when additional volume is below 9%, the A domains are swollen by the additional homopolymers, while the B domains remain the same in size as that in number 13 in Figure 2. We may notice from number I in Figure 4B that there is a very small A domain between two B domains. Number II in Figure 5 shows that this small A domain contains pure A blocks. The arrangement of A domains in this way guarantees the homogeneous distribution of the junction points around the B domain. With further increase of additional homopolymers, all A blocks will be distributed around the domains formed by homopolymers in order to fully cover the surface of domains formed by these homopolymers. Therefore, the small A domain, formed by pure A blocks, will disappear. Two B domains (green) will aggregate into a single bigger one, resulting in a new pattern as shown in number II in Figure 4B. Still, as the additional volume of homopolymers increases up to 19%, the A domains become so large that the A blocks cannot completely cover the whole surface. As a result, the system has to adjust its pattern, that is, two A domains aggregate into a big one to reduce the total surface area (number III in Figure 4B). For number III in Figure 4B, there are still redundant A blocks that do not need to cover all the homopolymer domains. Those redundant A blocks will form a small domain [small red one] between two B domains, resulting in the formation of smaller B domains [green].

With the further addition of homopolymer, the system will adjust itself to reduce the surface of the swollen A domain

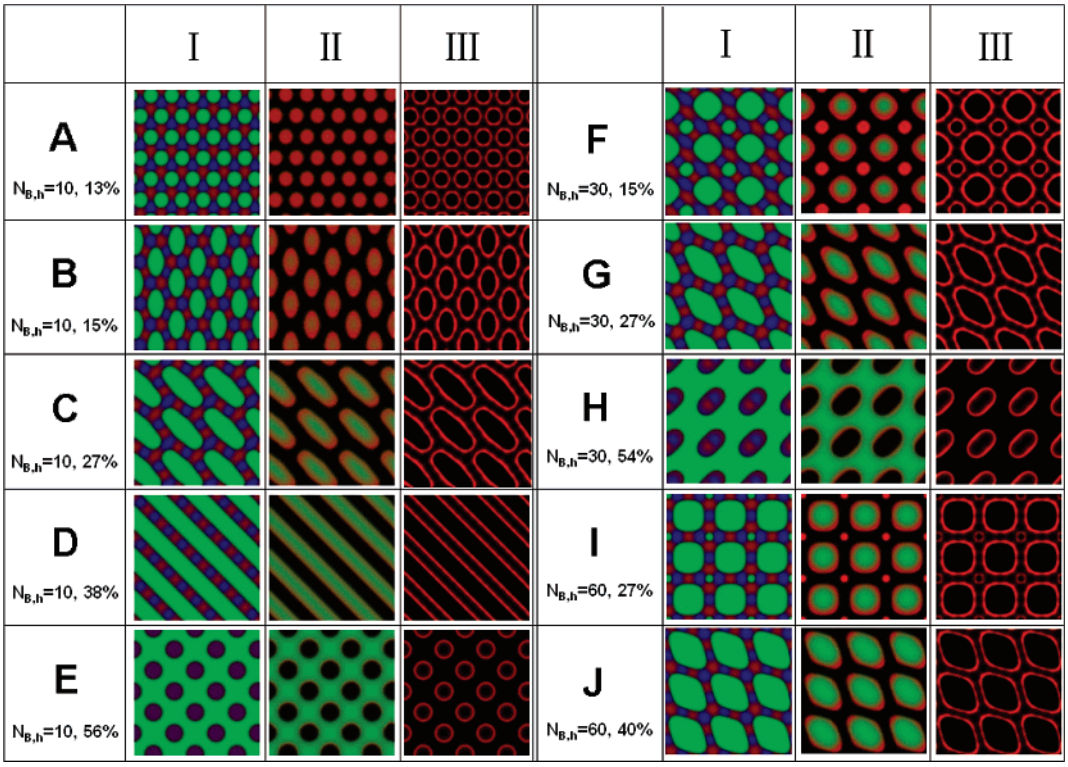

Figure 7. Density distribution of monomers belonging to the three kinds of component (I), A component (II), and junction points (III) after addition of different quantities of B homopolymers having varied molecular length ($N_{B,h}$). In column I, red, green, and blue represent A, B, and C components, respectively. In column II, green and red represent B homopolymer and B block on the ABC 3-miktoarm terpolymers, respectively.

allowing the surface to be fully covered. As a result, patterns as shown in numbers IV and V in Figure 4B are finally produced.

From Figure 4D,F, we understand, after the length of chain exceeds $N_{A,h} = 90$, that the microstructures do not depend on the linear homopolymer length, i.e., these three systems display the identical patterns, and the addition volume fraction scales corresponding to each patterns are almost the same. For the case of chain length $N_{homo,A} = 60$, some patterns such as numbers I, II, III, IV, and VII in Figure 4C also appear in Figure 4B, but other patterns such as numbers I, II, V, VI, and VII appear in Figure 4D,E.

3.2. Addition of B Homopolymers. The microstructures assembled via the mixtures of ABC 3-miktoarm star terpolymers and B homopolymers can be characterized by the following common features. First, these structures rely on both the volume fraction and length of homopolymers as the homopolymer is shorter than 30 segments, i.e., the length of the corresponding B blocks on the terpolymer (Figure 6A,B), but only on volume fractions if the homopolymer is longer (Figures 6C−E). Second, the junction points are still distributed homogeneously on the interfaces around the B domains (Figure 7). Third, the domains formed by pure B homopolymers are fully enclosed by the pure B blocks (Figure 7).

While adding the B homopolymers having a length as short as $N_{B,h} = 10$, all swollen B domains are an identical size, indicating swollen B domains are full of the equivalent quantity of B homopolymers (number I in Figure 6A). On the contrary, when adding homopolymers with longer length, not all the B domains contain B homopolymers. As the volume fraction of homopolymers is less than 15%, only half of the B domain is swollen into larger ones by the homopolymers, while another half of the B domain contains only pure B blocks (number I in Figure 6B−E and F in Figure 7). Further addition of B homopolymers into the system will consume more B blocks in order to fully cover the surfaces of domains formed by pure homopolymers. The patterns in number II in Figure 6C−E show that the domains formed by pure B blocks become small in size while the swollen B domains are enlarged, resulting in the formation of different patterns (number II of C−E in Figure 6) from those in number I in Figure 6C−E. In this system, the swollen B domains, which are usually diamond-like (numbers II of A and B and III of C−E in Figure 6), will aggregate into lamellas, having rectangle-like A and C domains that alternatively form a line between two lamellas (numbers III of A and B and IV of C−E in Figure 6), prior to the formation of continue phases (number V of A−E in Figure 6).

4. Conclusion

Microstructures of the mixtures of ABC 3-miktoarm star terpolymers and linear homopolymers are investigated using self-consistent mean-field theory (SCFT) in a two-dimensional space. For the pure ABC 3-miktoarm star terpolymer having three equal block lengths and interaction parameters $\chi_{AB}N = \chi_{BC}N = 2\chi_{AC}N = 36$, seven types of microstructures, such as hexagonal lattice, lamellar phases, hexagonal honeycomb lattice, broken lamellar phases, core/shell tetragonal lattice, interpenetrating tetragonal lattice, and disorder phases, were produced. Because of the high incompatibility of the B component with the other two components, the domains of the B component have a tendency to form in a circle-like structure to lower the system energy by reducing the contact area with the other two components; and the junction points were distributed homogeneously around domains of component B also to avoid the direct connection between components B with two other components in order to lower the system energy. The phase behaviors of pure ABC 3-miktoarm star terpolymers can be understood based on the above-mentioned two factors. Still, after addition of A and B homopolymers, to lower the free energies of the system, the B domain also tends to display in a circle-like or an ellipse-like structure, and the junction points are always distributed homogeneously on the interface around the B domain. The patterns of mixtures of ABC 3-miktoarm star terpolymer and homopolymers can also be understood based on the above-mentioned two factors.

Acknowledgment. We express our gratitude to the Outstanding Youth Fund (No. 20525416), the Programs of the National Natural Science Foundation of China (Nos. 20490220, 20374050, and 90403022), and the National Basic Research Program of China (No. 2005CB623800) for their financial support to this study.

References and Notes

(1) Hamley, I. W. *The Physics of Block Copolymers*; Oxford University Press: New York, 1998.
(2) Khandpur, A. K.; Foster, S.; Bates, F. S.; Hamley, I. W.; Ryan, A. J.; Almdal, K.; Mortensen, K. *Macromolecules* **1995**, *28*, 8796.
(3) Matsen, M. W.; Bates, F. S. *Macromolecules* **1996**, *29*, 1091. Matsen, M. W.; Bates, F. S. *J. Chem. Phys.* **1997**, *106*, 2436.
(4) Matsen, M. W. *J. Chem. Phys.* **2000**, *113*, 5539.
(5) Tyler, C. A.; Morse, D. C. *Phys. Rev. Lett.* **2005**, *94*, 208302.
(6) Mogi, Y.; Mori, K.; Matsushita, Y.; Noda, I. *Macromolecules* **1992**, *25*, 5412.
(7) Stadler, R.; Auschra, C.; Beckmann, J.; Krappe, U.; Voigtmartin, L.; Leibler, L. *Macromolecules* **1995**, *28*, 3080.
(8) Breiner, U.; Krappe, U.; Thomas, E. L.; Stadler, R. *Macromolecules* **1998**, *31*, 135.
(9) Goldacker, T.; Abetz, V. *Macromolecules* **1999**, *32*, 5165.
(10) Tang, P.; Qiu, F.; Zhang, H. D.; Yang, Y. L. *Phys. Rev. E* **2004**, *69*, 031803.
(11) Tang, P.; Qiu, F.; Zhang, H. D.; Yang, Y. L. *J. Phys. Chem. B* **2004**, *108*, 8434.
(12) Jiang, Y.; Yan, X. Y.; Liang, H. J.; Shi, A.-C. *J. Phys. Chem. B* **2004**, *109*, 21047.
(13) Winey, K. I.; Thomas, E. L.; Fetters, L. J. *Macromolecules* **1992**, *25*, 2645.
(14) Hadjuk, D. A.; Harper, P. E.; Gruner, S. M.; Honecker, C. C.; Kim, G.; Thomas, E. L.; Fetters, L. J. *Macromolecules* **1994**, *27*, 4063.
(15) Hashimoto, T.; Yamasaki, K.; Koizumi, S.; Hasegawa, H. *Macromolecules* **1993**, *26*, 2895.
(16) Zhao, J.; Majumdar, B.; Schulz, M. F.; Bates, F. S.; Almdal, K.; Mortensen, K.; Hajduk, D. A.; Gruner, S. M. *Macromolecules* **1996**, *29*, 1204.
(17) Lai, C.; Russel, W. B.; Register, R. A.; Marchand, G. R.; Adamson, D. H. *Macromolecules* **2000**, *33*, 3461.
(18) Matsen, M. W. *Macromolecules* **1995**, *28*, 5765.
(19) Whitmore, M. D.; Noolandi, J. *Macromolecules* **1985**, *18*, 2486.
(20) Lyatskaya, Yu. V.; Zhulina, E. B.; Birshtein, T. M. *Polymer* **1992**, *33*, 343.
(21) Spontak, R. J. *Macromolecules* **1994**, *27*, 6363.
(22) Matsen, M. W.; Bates, F. S. *Macromolecules* **1995**, *28*, 7298.
(23) Matsen, M. W. *Phys. Rev. Lett.* **1995**, *74*, 4225.
(24) Wickham, R. A.; Shi, A.-C. *Macromolecules* **2001**, *34*, 6487.
(25) Gemma, T.; Hatano, A.; Dotera, T. *Macromolecules* **2002**, *35*, 3225.
(26) Schultz, A. J.; Hall, C. K.; Genzer, J. *J. Chem. Phys.* **2002**, *117*, 10329.
(27) Lu, T.; He, X. H.; Liang, H. J. *J. Chem. Phys.* **2004**, *121*, 9702.
(28) Edwards, S. F. *Proc. Phys. Soc.* **1965**, *85*, 613.
(29) Helfand, E. *J. Chem. Phys.* **1975**, *62*, 999.
(30) Matsen, M. W.; Schick, M. *Phys. Rev. Lett.* **1994**, *72*, 2660.
(31) Noolandi, J.; Shi, A.-C.; Linse, P. *Macromolecules* **1996**, *29*, 5907.
(32) Drolet, F.; Fredrickson, G. H. *Phys. Rev. Lett.* **1999**, *83*, 4317.
(33) Drolet, F.; Fredrickson, G. H. *Macromolecules* **2001**, *34*, 5317.
(34) Fredrickson, G. H.; Ganesan, V.; Drolet, F. *Macromolecules* **2002**, *35*, 16.
(35) Bohbot-Raviv, Y.; Wang, Z.-G. *Phys. Rev. Lett.* **2000**, *85*, 3428.
(36) Sides, S. W.; Fredrickson, G. H. *J. Chem. Phys.* **2004**, *121*, 4974.
(37) Sides, S. W.; Fredrickson, G. H. *Polymer* **2003**, *44*, 5859.
(38) Tyler, C. A.; Morse, D. C. *Macromolecules* **2003**, *36*, 8184.
(39) He, X. H.; Huang, L.; Liang, H. J.; Pan, C. Y. *J. Chem. Phys.* **2003**, *118*, 9861.